frontiers | Frontiers in Earth Science

TYPE Review
PUBLISHED 16 May 2023
DOI 10.3389/feart.2023.1171200

Check for updates

OPEN ACCESS

EDITED BY
Richard Douglas Elmore,
University of Oklahoma, United States

REVIEWED BY
Bernard A. Housen,
Western Washington University, United States
Joshua M. Feinberg,
University of Minnesota Twin Cities, United States

*CORRESPONDENCE
Adrian R. Muxworthy,
adrian.muxworthy@imperial.ac.uk
Jack N. Turney,
j.turney20@imperial.ac.uk

RECEIVED 21 February 2023
ACCEPTED 01 May 2023
PUBLISHED 16 May 2023

CITATION
Muxworthy AR, Turney JN, Qi L, Baker EB, Perkins JR and Abdulkarim MA (2023), Interpreting high-temperature magnetic susceptibility data of natural systems.
Front. Earth Sci. 11:1171200.
doi: 10.3389/feart.2023.1171200

COPYRIGHT
© 2023 Muxworthy, Turney, Qi, Baker, Perkins and Abdulkarim. This is an open-access article distributed under the terms of the Creative Commons Attribution License (CC BY). The use, distribution or reproduction in other forums is permitted, provided the original author(s) and the copyright owner(s) are credited and that the original publication in this journal is cited, in accordance with accepted academic practice. No use, distribution or reproduction is permitted which does not comply with these terms.

Interpreting high-temperature magnetic susceptibility data of natural systems

Adrian R. Muxworthy[1,2]*, Jack N. Turney[1]*, Liang Qi[1], Evelyn B. Baker[1], Joseph R. Perkins[1] and Maryam A. Abdulkarim[1]

[1]Natural Magnetism Group, Department of Earth Science and Engineering, Imperial College London, London, United Kingdom, [2]Department of Earth Sciences, University College London, London, United Kingdom

High-temperature susceptibility (HT-χ) data are routinely measured in Earth, planetary, and environmental sciences to rapidly identify the magnetic mineralogy of natural systems. The interpretation of such data can be complicated. Whilst some minerals are relatively unaltered by heating and are easy to identify through their Curie or Néel temperature, other common magnetic phases, e.g., iron sulphides, are very unstable to heating. This makes HT-χ interpretation challenging, especially in multi-mineralogical samples. Here, we report a review of the HT-χ data measured primarily at Imperial College London of common magnetic minerals found in natural samples. We show examples of "near pure" natural samples, in addition to examples of interpretation of multi-phase HT-χ data. We hope that this paper will act be the first reference paper for HT-χ data interpretation.

KEYWORDS

high-temperature magnetic susceptibility, environmental magnetism, mineral magnetism, iron oxide, iron oxyhydroxide, iron sulphide, iron carbonate

1 Introduction

In Earth, planetary, and environmental sciences, magnetic techniques are often employed to rapidly measure the properties of rocks, sediments, meteorites, and soils. These magnetic properties can be proxies for formation environments or indicators of magnetic recording fidelity. The magnetic properties of samples are dependent on the magnetic mineralogy and grain size and shape of the minerals within. Unfortunately, there is no single measurement technique that provides a unique magnetic interpretation; a range of methods are applied, instead. To determine the magnetic mineralogy, samples are often heated to identify the Curie temperatures, Néel temperatures, and/or phase changes (Collinson, 1983). Other methods are available; however, these are often limited by accessibility, e.g., low-temperature thermomagnetometry (< 300 K), and magnetic mineral concentration, e.g., electron microscopy and Mössbauer spectroscopy (Evans and Heller, 2003).

Minerals have different responses to heating, with many common magnetic minerals displaying chemical alteration during heating (Minyuk et al., 2011; Till and Nowaczyk, 2018); this means that high-temperature thermomagnetometry does more than simply determining Curie (T_C) or Néel (T_N) temperatures. It is these chemical alteration products which can be used to identify the initial magnetic minerals in a sample, e.g., siderite is paramagnetic above room temperature, but forms magnetite on heating, aiding its identification (Housen et al., 1996; Abdulkarim et al., 2022a).

There are essentially two routine approaches in Earth sciences for analysing high-temperature behaviour: 1) measuring the high-field magnetisation as a function of temperature ($M_s - T$) or 2) high-temperature magnetic susceptibility (HT-χ) analysis. Both methods have benefits, e.g., the former approach is "superior", in that it directly determines T_C, whereas HT-χ behaviour near T_C is complicated by multiple processes, i.e., unblocking effects such as superparamagnetism (Fabian et al., 2013). HT-χ is also more sensitive to grain-size effects, e.g., larger superparamagnetic grains and multi-domain grains, which contribute to their behaviour more than single-domain grains (Fabian et al., 2013; Petrovský and Kapič;ka, 2006). However, due to a number of other factors, e.g., ease of use, commercial availability, instrument cost, and sample-size/sensitivity, HT-χ data are routinely measured in many laboratories worldwide; we suspect the majority.

In recent years, the Natural Magnetism Group at Imperial College London has used HT-χ analysis extensively in its study of a wide range of rock types, including basalts, ophiolite, and sedimentary rocks (Emmerton et al., 2013; Berndt and Muxworthy, 2017; Badejo et al., 2021b; Abdulkarim et al., 2022b). We have come up with procedures for identifying different minerals from HT-χ data. These interpretation procedures have been confirmed and fine-tuned through other analysis methods, e.g., Mössbauer spectroscopy, low-temperature magnetometry, electron microscopy, X-ray diffraction, and magnetic hysteresis analysis. When writing papers for peer-review, it has become clear that there is no single citable article which reviews the wide range of HT-χ behaviour of natural systems reported in the literature. Rather, the HT-χ behaviour of each mineral has to be individually cited. We think that a review of the interpretation of HT-χ data for common magnetic minerals would be helpful to the community.

In this paper, we provide a review of the interpretation of HT-χ data for natural samples. This is based primarily on not only the work undertaken at Imperial College London but also takes examples from the literature. We consider "near pure" natural samples, in addition to providing examples of how to interpret more complex signals. We consider iron oxides, iron oxyhydroxides, iron sulphides, iron carbonate, iron phosphate, and ferritchromites, plus titanium-substituted iron oxides. We have been unable to find natural examples of some minerals in a "near pure" state, e.g., maghemite; for such cases, we provide a typical example with interpretation.

2 HT-χ data "near pure" natural minerals

We provide examples for HT-χ data for common natural samples heated in argon atmosphere. We prefer heating in Ar to heating in air, as the latter tends to exaggerate the oxidation processes, making identification of the initial magnetic minerals harder, and is more sensitive to the heating rate (Jordanova and Jordanova, 2016); however, there are instances where HT-χ measured in air can be helpful, e.g., during rock magnetic analysis as part of paleointensity studies carried out in air. The minerals described are not meant to be exhaustive; there are many minerals not considered, e.g., ferrihydrite. We consider all the magnetic minerals that we have routinely observed. In nearly all cases, supporting evidence for the mineral classification of each sample, e.g., Mössbauer spectroscopy, is in the references provided. In the few cases where it is not, e.g., the hematite sample (**Figure 1**), the samples had clear mineral characteristics and showed good HT-χ behaviour, i.e., agreed with previously published results. The primary focus of this review paper is to describe the HT-χ behaviour pictorially, i.e., if a sample displays reversible HT-χ behaviour with a clear T_C, we will provide less text description, e.g., magnetite (**Figure 1A**). Measurements were made using AGICO CS2 or CS3 systems fitted to different types of Kappabridges at various laboratories, including Imperial College London. To obtain absolute magnetic susceptibility values, we recommend measuring samples with known shapes, volumes, and masses using a Kappabridge in the "bulk" sample mode.

Curie and Néel temperatures observed in the manuscript may not exactly match those quoted in the literature (Dunlop and Özdemir, 1997). There are two major reasons: 1) all the samples reported here are natural, meaning that some impurities may exist and 2) it is well-documented that HT-χ approaches for determining T_C or T_N are compromised due to low-field effects, e.g., superparamagnetism and domain-wall unblocking, which are not present in M_s-T data (Fabian et al., 2013). This behaviour near T_C or T_N "distorts" the accurate determination of T_C and T_N during HT-χ analysis, which as a result of this, are often overestimated (Petrovský and Kapič;ka, 2006; Fabian et al., 2013). The Curie and Néel temperature estimates made in this paper are approximate and are performed by eye and are accurate to within ±5 °C at best. To obtain accurate T_C and T_N estimates it is necessary to measure the M_s-T data (Petrovský and Kapič;ka, 2006; Fabian et al., 2013).

2.1 Iron oxides

HT-χ data for magnetite (Fe_3O_4), maghemite (γ-Fe_2O_3), and hematite (α-Fe_2O_3) are shown in **Figure 1**. The magnetite sample is sample E (150 μm) obtained from a greenschist in Shetland, United Kingdom, described by Muxworthy (1998) and Muxworthy and McClelland (2000) (**Figure 1A**). Notably, the sample used to measure the HT-χ was not treated using the *carbonate–bicarbonate–dithionite* method (Hunt et al., 1995), unlike the E (150 μm) sample referenced in Muxworthy and McClelland (2000).

Maghemite is very common; however, pure maghemite rarely occurs in nature. As maghemite is often a low-temperature oxidation product of magnetite (Bleil and Petersen, 1983), it is usually found in the presence of magnetite (Gehring et al., 2009). Maghemite is also commonly found in the presence of additional non-magnetic minerals that form magnetite during HT-χ analysis (Oches and Banerjee, 1996). We provide an example of maghemite HT-χ behaviour, in the presence of magnetite, in **Figure 1B**; the sample is obtained from the sandstone interval of the Pentland Formation from the Inner Moray Firth, North Sea (Perkins, 2022; Perkins et al., 2023). Maghemite inverts to hematite on heating, leading to a drop in susceptibility as the spontaneous magnetisation of maghemite is ~150× greater than that of hematite Dunlop and Özdemir (1997). This process usually occurs at 300 °C–400 °C, although, in rare samples, it can occur at higher temperatures > 600 °C (Özdemir, 1990). In **Figure 1B**, at temperatures >500 °C, there is a secondary peak. This secondary peak is likely a combination of two processes: 1) the formation and presence of magnetite,

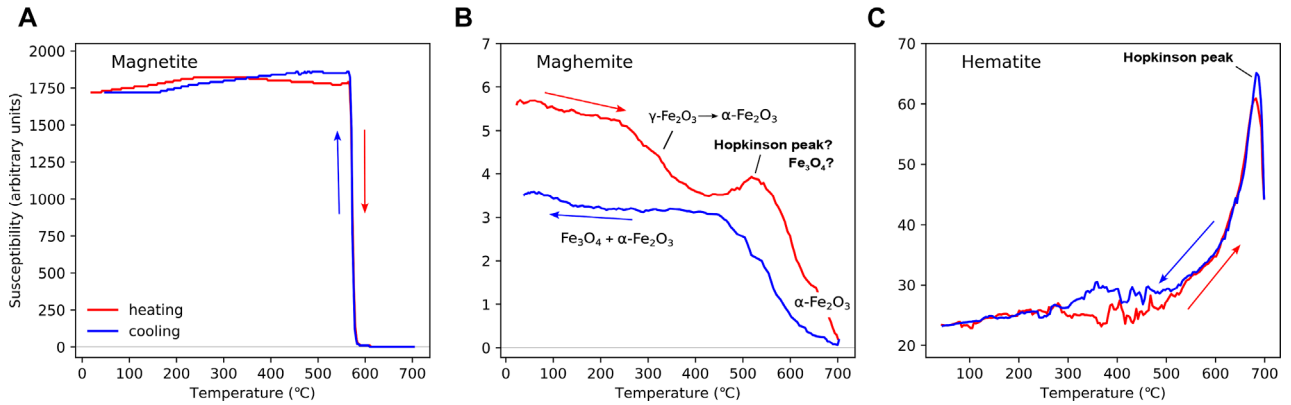

FIGURE 1
HT-χ data for **(A)** the magnetite (Fe_3O_4 sample described in Muxworthy, 1998; Muxworthy and McClelland, 2000); **(B)** maghemite (γ-Fe_2O_3) from Well 12/27–1 (depth 3,738.9 ft) in the Inner Moray Firth, North Sea (Perkins, 2022; Perkins et al., 2023); and **(C)** hematite (α-Fe_2O_3, unpublished). In **(B)**, some magnetite formation observed during the experiment is shown. Heating for all three samples was carried out in Ar. For **(A)** the Kappabridge settings were as follows: heating rate = 10 °C/min, field = 300 A/m, and frequency 920 Hz; and for **(B)** and **(C)**, the Kappabridge settings were as follows: heating rate = 13.7 °C/min, field = 200 A/m, and frequency 976 Hz.

which was likely formed during the HT-χ experiment and 2) Hopkinson-peak effects (Hopkinson, 1889). Hopkinson peaks are usually associated with the unblocking of single-domain grains making them superparamagnetic or increased domain wall motion in larger multi-domain grains due to enhanced thermal energy; both mechanisms cause an increase in χ, though this is particularly enhanced in fine single-domain grains (Fabian et al., 2013). On heating above this secondary peak, χ continues to decrease to the Néel temperature of hematite. This hematite is likely formed during the HT-χ experiment from the inversion of the original maghemite. On cooling, both the hematite phase plus magnetite and possibly maghemite are not inverted during the experiment. Similar HT-χ behaviour is widely reported for maghemite (Oches and Banerjee, 1996; Gao et al., 2019); however, given that maghemite rarely occurs as a single phase and its inversion temperature is variable (Özdemir, 1990), maghemite can display a wide range of HT-χ behaviours.

The hematite sample used to measure the HT-χ curve shown in **Figure 1C** is a piece of botryoidal hematite obtained from the Western Sahara, Morocco. The data are previously unpublished. The sample has a Hopkinson peak below 700 °C, but the susceptibility does not reduce to 0 by 700 °C; 700 °C is the maximum temperature possible in the AGICO CS3 system used to measure this sample. The standard T_N for hematite as quoted in the literature on rock magnetism is 680 °C–690 °C determined using the M_s-T data (Bleil and Petersen, 1982; Özdemir and Dunlop, 2005). The higher T_N behaviour observed here is likely due to HT-χ data yielding over-estimates of T_N Fabian et al. (2013), in addition to it being a natural sample with a high T_N; T_N determined for this sample from the second derivative of the M_s-T data measured using a Princeton vibrating sample magnetometer was estimated at ~699 °C ±5 °C. This high T_N is likely due to a high Fe:O ratio in the sample. Both Minyuk et al. (2011) and Cunha et al. (2017) reported similar HT-χ curves for "near pure" natural hematite. However, when hematite is mixed with other minerals, it can also display HT-χ signatures like those seen in **Figure 1B**, i.e., above ~600 °C, hematite is the only contributing phase with a gradual decrease in χ up to its Néel temperature at ~680 °C.

2.2 Titanium-rich iron oxides

Titanium-rich iron oxide is the general name describing a range of solid solutions with various proportions of iron, titanium, and oxygen (Haggerty, 1991; Dunlop and Özdemir, 1997). We only focus here on the titanomagnetite "TM60" ($Fe_{2.4}Ti_{0.6}O_4$) and its oxidation product titanomaghemite TMH60 and the hematite variant TH60. Clearly, there are a range of intermediate states of Ti and oxidative states; however, we concentrate on TM60 due to it being very common in nature, being particularly dominant in oceanic basalts. Oceanic TM60 slowly oxidises to TMH60 over millions of years (Bleil and Petersen, 1983; Krása and Matzka, 2007).

In **Figure 2A** we show a typical TM60 example for a sample obtained from the 1991 eruption of Hekla, Iceland (Muxworthy, 2010; Muxworthy et al., 2011). The sample has a clear peak at $T < 200$ °C, with a T_C just below 200 °C, which is indicative of TM60 (O'Reilly, 1976). There is also a smaller T_C close to 580 °C, which is indicative of magnetite. TM60 rarely occurs as a single phase in rocks. This is because in the formation of TM60, the larger iron-rich crystals precipitate first, attracting higher levels of Ti; the secondary smaller iron-rich crystals, i.e., <100 nm, which are often inclusions, attract less Ti and are closer to "pure" magnetite (Almeida et al., 2014). The result is the larger iron oxide crystals which have higher Ti content than the smaller ones. The HT-χ behaviour of intermediate titanomagnetites, i.e., TM0–TM60, has been reported to be complex with a thermal history dependency (Jackson and Bowles, 2018).

The HT-χ data for a TMH60 sample obtained from Deep Sea Drilling Project Leg 73 Hole 519A are shown in **Figure 2**. This sample has an oxidation parameter of ~0.8 (Petersen, 1984), so it is not a pure TMH60 sample, but close to and "typical" for natural titanomaghemites. On heating, TMH60 exsolves to magnetite and ilmenite above ~300 °C Özdemir (1987). The HT-χ curve has a low temperature (<200 °C) associated with TMH60 and a second peak associated with the newly formed magnetite close to the T_C of magnetite. This behaviour is different to the behaviour of maghemite, which forms hematite on heating (**Figure 1B**).

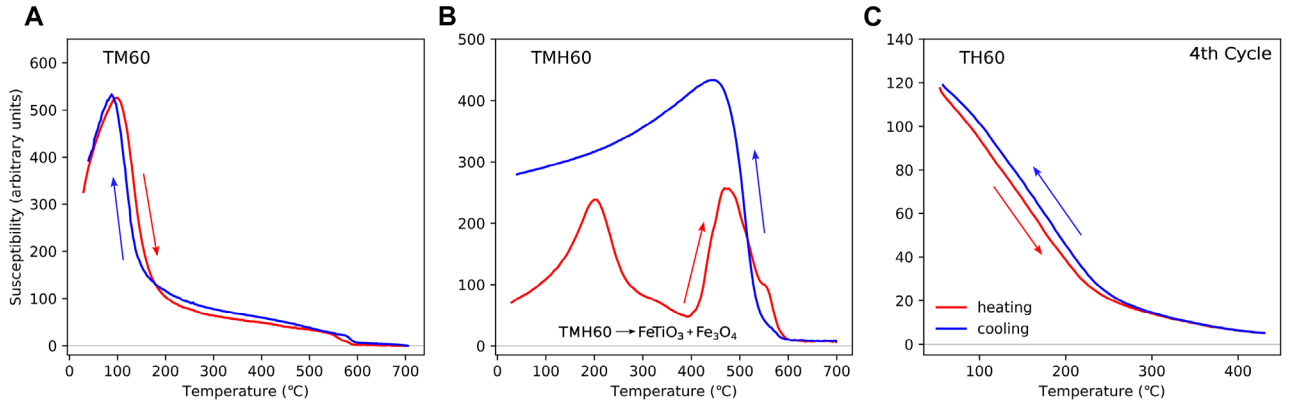

FIGURE 2
HT-χ data for titanium-rich iron oxides: **(A)** a titanomagnetite sample ($Fe_{2.4}Ti_{0.6}O_4$, TM60, sample H291B) from the 1991 eruption of Hekla, Iceland, described in Muxworthy (2010); Muxworthy et al. (2011); **(B)** a titanomaghemite sample (~TMH60, oxidation parameter ~0.8) from DSDP Leg 73 Hole 519A (Petersen, 1984); and **(C)** titanohematite (~TH60, sample 14SCA1-3ext2) from Hell Creek, Montana, United States (Sprain et al., 2016). HT-χ data for **(C)** is the final cycle of multi-cycled heating with peak temperatures every 100 °C, ending at 400 °C. Each cycle was reversible. A sister sample heated in air to 700 °C showed a similar behaviour; however, the cooling behaviour for this sister sample was irreversible, with a drop in susceptibility below 400 °C (Sprain et al., 2016). The HT-χ data in **(A)** and **(B)** are not previously published, but the samples are described in the cited references. Heating for all three samples was carried out in Ar. For **(A)** and **(C)** the Kappabridge settings were as follows: heating rate = 10 °C/min, field = 300 A/m, and frequency 920 Hz; and for **(B)**, the Kappabridge settings were as follows: heating rate = 13.7 °C/min, field = 200 A/m, and frequency 976 Hz.

Hematite is a canted antiferromagnetic; however, with the substitution of Ti, it becomes ferrimagnetic in the range α-$Fe_{2-y}Ti_yO_3$ for $0.5 < y < 0.7$, i.e., ~TH60 (Dunlop and Özdemir, 1997; Sprain et al., 2016). Titanohematite is reported in silicic lavas, pyroclastic deposits, and sedimentary rocks (Heller, 1980; Sprain et al., 2016), and is often associated with self-reversal processes (Nagata, 1952). For the titanohematite example, we show HT-χ data measured by Sprain et al. (2016) for magnetic extracts of Cretaceous–Paleogene sediments obtained from the Hell Creek region in Montana, United States (**Figure 2C**). They determined compositions ranging from y =0.53–0.63 using X-ray diffraction (XRD) and electron microprobe analysis. The samples display gradual decreases in χ, with a T_C ~200 °C–250 °C.

2.3 Iron oxyhydroxides

In **Figure 3A**, we show HT-χ behaviour of a natural goethite (α-FeOOH) sample from Well 11/30a-8 from the Inner Moray Firth in the North Sea (Perkins et al., 2023). Goethite has distinctive HT-χ behaviour, dehydrating from goethite to hematite on warming; however, some goethite transform via an intermediate magnetite phase in the range ~ 300 °C–400 °C (Özdemir and Dunlop, 2000). Because magnetite is magnetically much stronger than goethite and hematite, there is a distinctive magnetite "bump" in the HT-χ curve. This magnetite phase is typically unstable and oxidizes to hematite on further heating. The resultant cooling curve has a higher χ than the original warming curve below 250 °C. This is because the newly formed hematite has a higher χ than goethite. Similar data have been reported in the literature (Minyuk et al., 2011).

Lepidocrocite (γ-FeOOH) dehydrates to maghemite on heating to ~200 °C–300 °C (Gendler et al., 2005). This maghemite phase is very unstable and inverts to hematite on further heating to ~400 °C–500 °C **Figure 3B**. The lepidocrocite sample shown in **Figure 3B** is obtained from Well 12/27–2 (depth 5190.6 ft) from the Inner Moray Firth in the North Sea (Perkins et al., 2023).

Other iron oxyhydroxides exist, e.g., ferrihydrite; however, these are generally very unstable and rapidly convert to fully ordered iron oxides and oxyhydroxides (Bilardello et al., 2020), and are not considered here.

2.4 Iron sulphides

Iron sulphides are common in anoxic environments, in particular sediments. We consider pyrite, greigite, and pyrrhotite. There are several other iron sulphides, but these are most common in terrestrial systems. Pyrite is paramagnetic, however, it is very stable and abundant in sulphur-rich systems and is important to identify and quantify in the iron cycle (Roberts, 2015). The pyrite (FeS_2) sample shown in **Figure 4A** is from Well 12/25–3 (depth 5600 ft) from the Moray Firth, North Sea (Perkins et al., 2023). Pyrite shows minimal change on heating to 700 °C (**Figure 4A**), although in some cases, it may convert to magnetite above 380 °C (Li and Zhang, 2005). On cooling, χ remains low before sharply increasing at ~320 °C (**Figure 4A**), due to change of pyrite to pyrrhotite (Li and Zhang, 2005; Wang et al., 2008).

Greigite forms as an intermediate phase along the pyrite reaction pathway (Berner, 1967; Hunger and Benning, 2007; Turney et al., 2023). Its ferrimagnetic properties make its identification critical for palaeomagnetic studies of shallow sediments (Snowball and Thompson, 1988; Chen et al., 2021). The sample in **Figure 4B** is a fine-grained marine mudstone from the Erhjen-chi section in southwestern Taiwan (Horng et al., 1992a; b). Greigite displays a Hopkinson peak between 240 °C and 250 °C during heating, followed by a sharp decrease in χ at ~400 °C (**Figure 4B**). Magnetite may form due to thermal alteration, i.e., from the decrease and increase in χ at 580 °C, as observed on the heating and cooling curves (**Figure 4B**). Cooling HT-χ curves often display evidence for

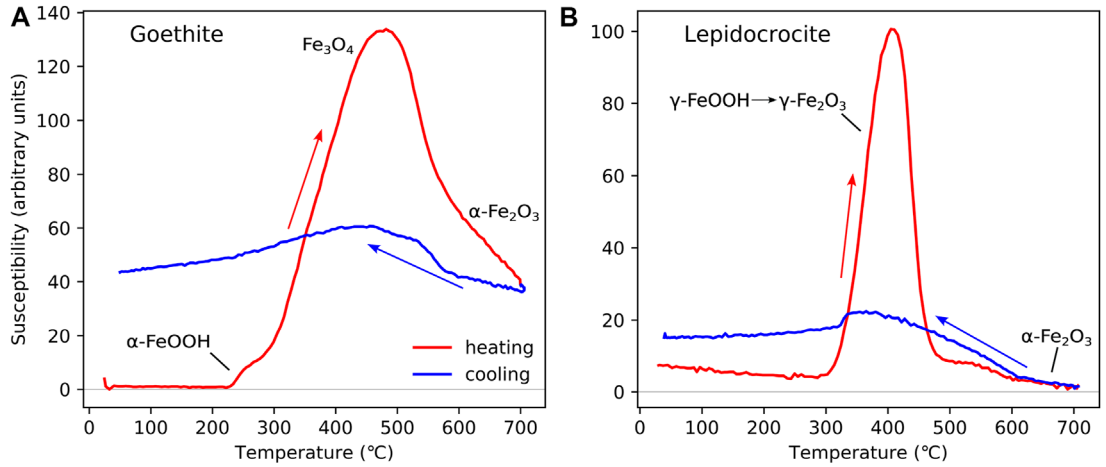

FIGURE 3
HT-χ data for "near pure" samples of: **(A)** goethite (α-FeOOH) and **(B)** lepidocrocite (γ-FeOOH). Both samples are from Inner Moray Firth, North Sea, United Kingdom (Perkins, 2022; Perkins et al., 2023). The goethite sample is from well 11/30a-8 (depth 6925.5 ft) and the lepidocrocite sample from well 12/27–2 (depth 5190.6 ft). Heating for both samples was carried out in Ar, with Kappabridge settings: heating rate = 13.7 °C/min, field = 200 A/m, and frequency 976 Hz.

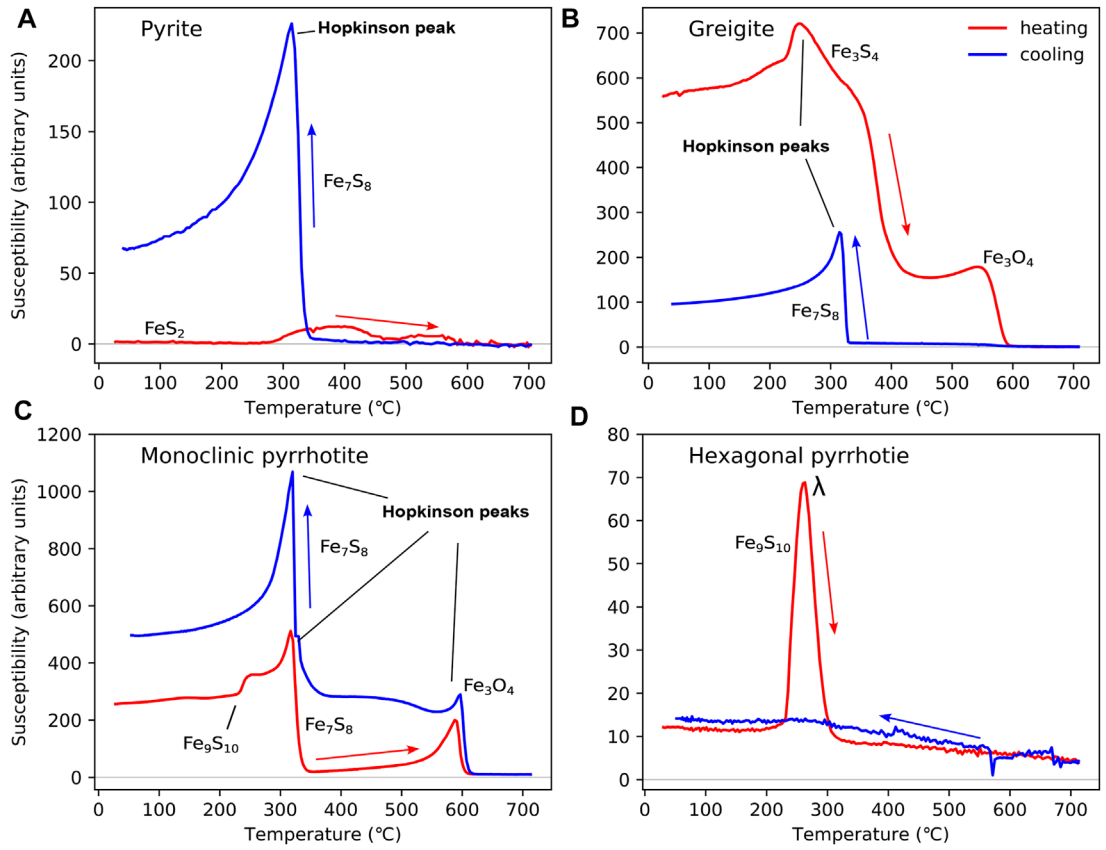

FIGURE 4
HT-χ data for iron sulphides, including **(A)** pyrite from Well 12/25–3 (depth 5,600 ft) in the North sea (Perkins et al., 2023); **(B)** greigite from marine mudstones of the Erhjen-chi section, SW Taiwan (sample EJC22) (Horng et al., 1992b; a; Roberts et al., 2011); **(C)** monoclinic pyrrhotite (sample 564 m); and **(D)** hexagonal pyrrhotite (sample 8,080 m) from medium-grade metamorphic rocks of Central Europe (Kontny et al., 2000). All samples have been heated in Ar. For **(A)**, the Kappabridge settings were as follows: heating rate = 13.7 °C/min, field = 200 A/m, and frequency 976 Hz; and for **(C)** and **(D)**, the Kappabridge settings were as follows: heating rate = 8 °C–10 °C/min, field = 300 A/m, and frequency 920 Hz. The HT-χ settings for **(B)** are unknown.

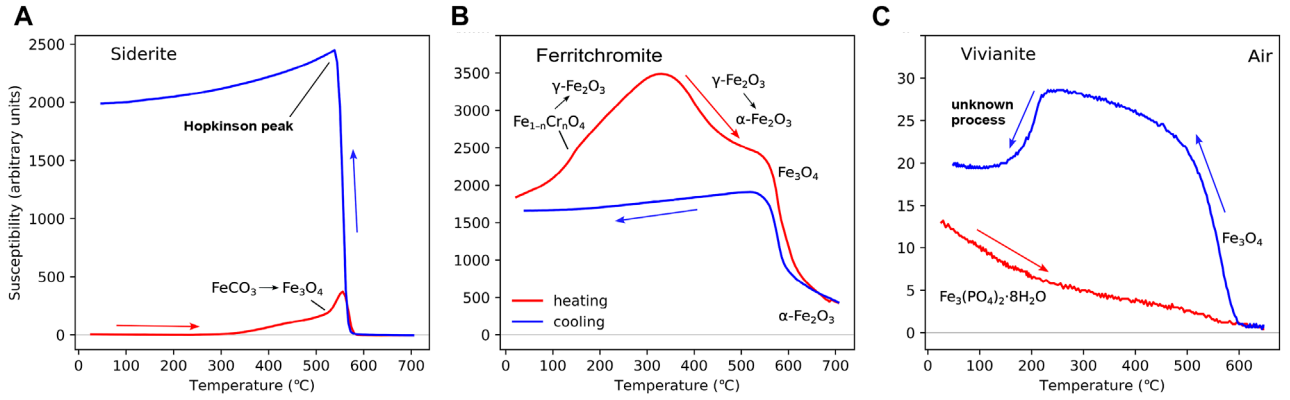

FIGURE 5
Example of HT-χ for "near pure" samples of **(A)** siderite ($FeCO_3$), **(B)** a ferritchromite sample, and **(C)** vivianite. The siderite example in **(A)** is sample S63654 from well 21/29a-08 from the Western Central Graben in the Central North Sea (Badejo et al., 2021a). The ferritchromite sample in **(B)** is from the Troodos Ophiolite, Cyprus (unpublished); the presence of ferritchromite was determined with energy-dispersive spectroscopy. Samples **(A)** and **(B)** were heated in Ar, with Kappabridge settings: heating rate = 13.7 °C/min, field = 200 A/m, and frequency 976 Hz. The vivianite sample in **(C)** is from the Priest River near Samuels, Idaho, United States, and is reproduced from Doctor and Feinberg (2022) who conducted heating in air. Kappabridge settings for **(C)**: heating rate = 11.8 °C/min, field = 300 A/m, and frequency 920 Hz, measured in air.

monoclinic pyrrhotite at ~320 °C (**Figure 4C**). This HT-χ behaviour for greigite is "ideal"; greigite commonly displays a wide range of HT-χ behaviours and is often found in the presence of abundant pyrite which dominates the HT-χ response (Roberts and Weaver, 2005; Badejo et al., 2021a). This high variability in HT-χ behaviour makes identifying the presence of greigite difficult (Roberts et al., 2011). Another example of typical greigite behaviour is discussed as follows.

The HT-χ behaviour of pyrrhotite depends on its stoichiometry (Kontny et al., 2000). We give examples for its two most common forms: 1) monoclinic pyrrhotite (Fe_7S_8, **Figure 4C**) and 2) hexagonal pyrrhotite (Fe_9S_{10}, **Figure 4D**). Both forms are from medium-grade amphibolite-facies metamorphic rocks of the Variscan basement complex in Central Europe (Kontny et al., 2000). Monoclinic pyrrhotite is ferrimagnetic at ambient temperatures, but becomes unstable at high temperatures, with a T_C of ~325 °C (Schwarz and Vaughan, 1972; Kontny et al., 2000) (**Figure 4C**). In contrast, hexagonal pyrrhotite is antiferromagnetic at room temperature; however, on heating, it becomes ferrimagnetic (at ~200 °C), with a T_C between 265 °C and 295 °C (Rochette et al., 1990) (**Figure 4D**). This transition is often referred to as the λ transition (Schwarz and Vaughan, 1972).

2.5 Other iron phases

The HT-χ behaviour of siderite ($FeCO_3$) is well-documented (Housen et al., 1996). Here, we provide an example from the Western Central Graben in the Central North Sea, United Kingdom (**Figure 5A**) (Badejo et al., 2021a). On heating, siderite converts to magnetite (above 400 °C–500 °C). On cooling, through T_C for magnetite, there is normally evidence for a significant increase in magnetite content.

Ferritchromite ($Fe_{1-n}Cr_nO_4$) is a Cr–Fe spinel phase with $0.1<n<0.6$, commonly found in serpentinised ultramafic and mafic rocks (Kądziałko-Hofmokl et al., 2008; Hodel et al., 2020). Here, we report the HT-χ data for an unpublished sample from the Troodos Ophiolite, Cyprus (**Figure 5B**). In natural samples, ferritchromite rarely occurs in a pure form and is normally found in the presence of iron oxides. There is an increase in the gradient of the HT-χ curve when heating between 100 °C and 150 °C, indicating the presence of ferritchromite as it destabilises to maghemite (Hodel et al., 2020). Above this temperature range, the presence of a mixture of maghemite and magnetite is observed (**Figure 1**). The presence of ferritchromite in this sample was determined via energy-dispersive spectroscopy. Ferritchromite with $0.1<n<0.2$ does not display this behaviour and displays reversible HT-χ behaviour with a T_C of ~520 °C (Kądziałko-Hofmokl et al., 2008).

Vivianite ($Fe_3(PO_4)_2{\cdot}8H_2O$) is a hydrated iron phosphate mainly found in anoxic lacustrine sediments (e.g., Rothe et al., 2015). Its importance is becoming increasingly recognised (e.g., Abdulkarim et al., 2022b). Vivianite is antiferromagnetic and is typically identified by low-temperature magnetic measurements, displaying a T_N of 12 K (Frederichs et al., 2003). The HT-χ data in the literature are very limited (Minyuk P. S. et al., 2013; Doctor and Feinberg, 2022). The example used here is for a large single crystal (5 cm long) collected along the Priest River near Samuels, Idaho, United States and its HT-χ measured in air, carried out by Doctor and Feinberg (2022) (**Figure 5C**). The sample is close to "pure" vivianite as determined by microprobe analysis. On heating, the susceptibility decreases with temperature as expected for a paramagnet. On cooling, a magnetite-like phase is seen to form, but on further cooling, there is a sharp drop in χ below 200 °C. Minyuk P. S. et al. (2013) reported similar curves for natural vivianite, but only after conducting two or three heating cycles in air. Minyuk P. S. et al. (2013) showed the drop at ~200 °C on cooling to be reversible.

Of all the minerals reported in this paper, the alteration of vivianite during heating is perhaps the least understood. Whilst it is well-documented that vivianite dehydrates over a range of discrete temperatures up to 437 °C, the origin of further changes above 600 °C is open to debate: Are they dehydration or oxidation processes? (Dormann et al., 1982; Rodgers and Henderson, 1986; Frost et al.,

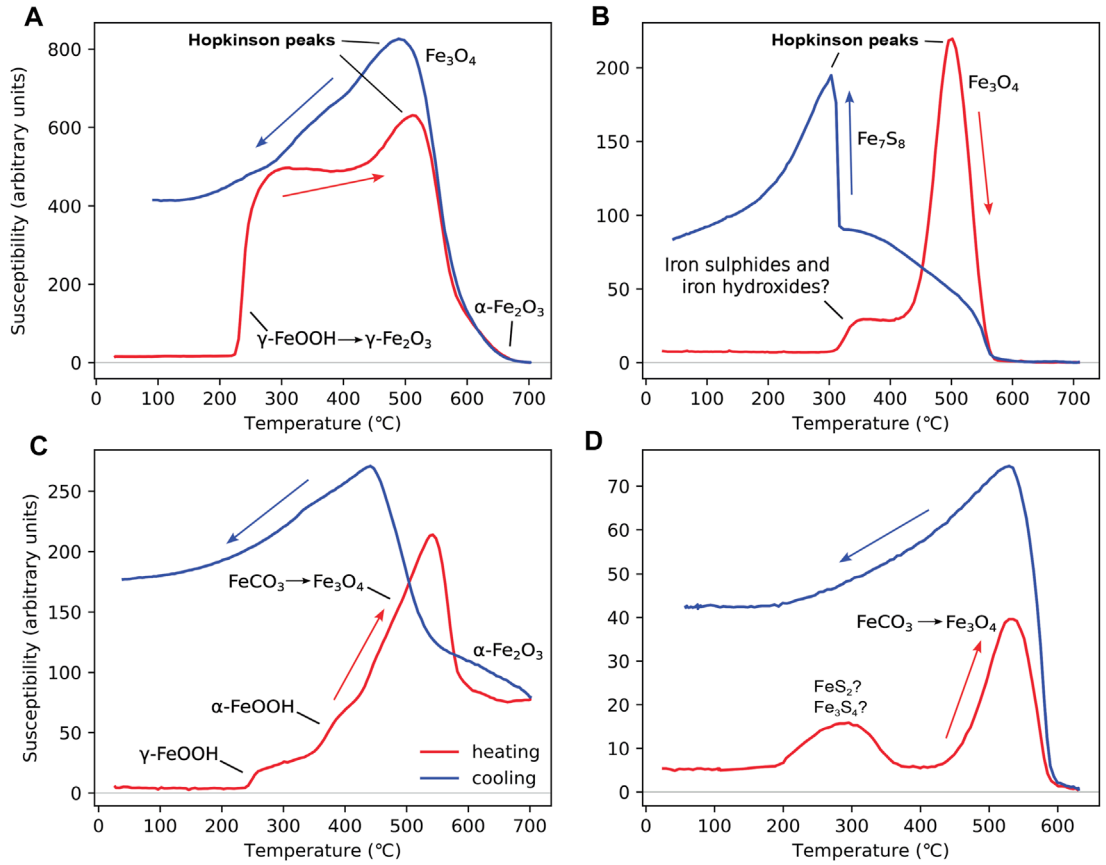

FIGURE 6
HT-χ data for samples with mixed mineralogies: **(A)** a shale sample (S-1428) from the Catcher field in the North Sea (Abdulkarim et al., 2022b); **(B)** sample 211–1 from Well 211/29-C4 (depth 3422 m) in the Brent oil field, North Sea (Emmerton, 2013); **(C)** sample from well 12/21–4 (depth 6,755.0 ft) in the Inner Moray Firth, North Sea (Perkins, 2022; Perkins et al., 2023); and **(D)** a salt marsh sample (NF4A) from the Warham salt marsh, Norfolk, United Kingdom (unpublished). Heating for all samples was carried out in Ar, with Kappabridge settings: heating rate = 13.7 °C/min, field = 200 A/m, and frequency 976 Hz.

2003; Ogorodova et al., 2017) Nevertheless, there is no evidence that these further structural changes lead to the formation of magnetite. What appears more likely, as suggested by Minyuk P. S. et al. (2013), is that vivianite produces reducing conditions, which leads to the formation of magnetite possibly from hematite. Further work is required to identify the origin of the decrease observed on cooling below 200 °C.

3 Examples of interpreting multi-phase HT-χ data

Multi-phase samples are common in nature. In this section, we provide some examples of how we interpret the HT-χ data for multi-phase samples. Interpretation of the HT-χ data is often aided by other magnetic data or information, e.g., is the area rich in sulphur or not; many iron sulphides and oxyhydroxides alter on heating, forming more magnetic phases; knowing whether these are due to sulphur can be highly beneficial.

Figure 6A shows a shale sample (S-1428) from the Burgman field in the North Sea (Abdulkarim et al., 2022b). This sample contains significant levels of lepidocrocite indicated by the formation of a higher magnetisation phase, i.e., maghemite, at ~230 °C. A second magnetic phase forms on further heating above ~450 °C. This second phase is likely magnetite. Above 600 °C, hematite is observed. The cooling curve suggests a mixture of hematite and magnetite. Abdulkarim et al. (2022b) interpreted this second phase as being either goethite or greigite based on the HT-χ data alone; the indication of hematite could come from dehydration of goethite or from the inversion of maghemite in the γ-FeOOH $\rightarrow \gamma$-Fe_2O_3 $\rightarrow \alpha$-Fe_2O_3 transition. On combining the HT-χ data with low-temperature and hysteresis data, Abdulkarim et al. (2022b) concluded that this second phase was greigite.

Sample 211–1 from Well 211/29-C4 (depth 3,422 m) in the Brent oil field, North Sea (**Figure 6B**), is a "dry" (unstained by oil) sandstone (Emmerton, 2013). The sample contains a mixture of pyrite (and possibly greigite) and goethite (or another phase that forms unstable intermediate magnetite). The pyrite forms pyrrhotite on heating (**Figure 4A**), and possibly some magnetite, and goethite forms hematite with some intermediate unstable magnetite (**Figure 3A**). Low-temperature analysis of this sample also found evidence for magnetite (Emmerton, 2013); however, there is little evidence for original magnetite in the HT-χ data.

In **Figure 6C**, we consider a sample from the Inner Moray Firth, North Sea (Perkins, 2022; Perkins et al., 2023). The sample contains lepidicrocite, goethite, and siderite. Lepidicrocite is identified by the small increase in χ at $T < 300$ °C (**Figure 3B**); however, the formation of magnetite from goethite and siderite at $T > 300$ °C starts to dominate the signal (**Figures 3A**; **5A**). At $T > 600$ °C, there is clear evidence for the presence of hematite. On cooling, there is an increase in the magnetite signal, which is indicative of a non-iron hydroxide phase. Perkins (2022) and Perkins et al. (2023), with limited evidence for iron sulphides in this well, interpreted this magnetite-producing phase as siderite.

In **Figure 6D**, we consider a sample from the Warham salt marsh in Norfolk, United Kingdom. Samples from this area have been previously shown to contain greigite, siderite, and pyrite using XRD (Pye, 1981; Lin et al., 2019). The "bump" between ~200°C and ~350°C is likely due to greigite; decreases in χ at ~350 °C have been reported in synthetic and natural greigite samples (Minyuk P. et al., 2013). Multi-cycle curves found this "bump" to be irreversible >300°C, suggesting alteration. Siderite is identified by the increase at $T > 450$ °C, as siderite alters to magnetite at high temperatures (**Figure 5A**).

4 Conclusion

In this short paper, we have provided examples of HT-χ behaviour for many of the magnetic minerals commonly found in nature, i.e., iron oxides and iron sulphides; however, the list is not exhaustive. It is clear from the examples given that interpreting HT-χ data can be challenging and non-unique. For example, many minerals form magnetite on heating (**Figures 2–5**) and some minerals, e.g., vivianite and greigite, do not have consistent and distinctive HT-χ behaviour. To interpret such HT-χ data often requires additional information either gleaned through magnetic measurements or other means, e.g., is sulphur present? The Natural Magnetism Group often supplements HT-χ data with low-temperature magnetometry data, Mössbauer spectra, and electron microscopy images on select samples. Finally, in **Figure 6**, we provide some examples of how the Natural Magnetism Group interprets the HT-χ data.

Data availability statement

The data for this paper is available from zenodo.org. doi: 10.5281/zenodo.7904069.

Author contributions

JT, JP, and AM contributed to conception of the review. All members helped to decide which data to include. AM wrote the first draft of the manuscript, while JT, LQ, and EB wrote sections. JT drew the figures. All authors contributed to manuscript revision, read, and approved the submitted version. All authors listed have made a substantial, direct, and intellectual contribution to the work and approved it for publication.

Funding

EB acknowledges a UK Science and Technology Facilities Council PhD scholarship (STFC/2295497), JP (EP/R513052/1) and JT (EP/T51780X/1) acknowledge UK Engineering and Physical Sciences Research Council PhD scholarships, and MA acknowledges a Nigerian Petroleum Technology Development Fund PhD scholarship. AM acknowledges support from the UK Natural Environmental Research Council grant NE/V001388/1.

Acknowledgments

The authors would like to thank Tony Morris for the motivation behind this paper. The authors would also like to thank Agnes Kontny, David Krása, Nikolai Petersen, and Courtney Sprain for providing data or samples.

Conflict of interest

The authors declare that the research was conducted in the absence of any commercial or financial relationships that could be construed as a potential conflict of interest.

Publisher's note

All claims expressed in this article are solely those of the authors and do not necessarily represent those of their affiliated organizations, or those of the publisher, the editors, and the reviewers. Any product that may be evaluated in this article, or claim that may be made by its manufacturer, is not guaranteed or endorsed by the publisher.

References

Abdulkarim, M. A., Muxworthy, A. R., Fraser, A., Neumaier, M., Hu, P. X., and Cowan, A. (2022a). Siderite occurrence in petroleum systems and its potential as a hydrocarbon-migration proxy: A case study of the catcher area development and the bittern area, UK North Sea. *J. Petroleum Sci. Eng.* 212, 110248. doi:10.1016/j.petrol.2022.110248

Abdulkarim, M. A., Muxworthy, A. R., Fraser, A., Sims, M., and Cowan, A. (2022b). Effect of hydrocarbon presence and properties on the magnetic signature of the reservoir sediments of the catcher area development region, UK North Sea. *Front. Earth Sci.* 10. doi:10.3389/feart.2022.818624

Almeida, T. P., Muxworthy, A. R., Williams, W., Kasama, T., and Dunin-Borkowski, R. (2014). Magnetic characterization of synthetic titanomagnetites: Quantifying the recording fidelity of ideal synthetic analogs. *Geochem. Geophys. Geosystems* 15, 161–175. doi:10.1002/2013GC005047

Badejo, S. A., Muxworthy, A. R., Fraser, A., Neumaier, M., Perkins, J. R., Stevenson, G. R., et al. (2021a). Using magnetic techniques to calibrate hydrocarbon migration in petroleum systems modelling: A case study from the lower tertiary, UK central North Sea. *Geophys. J. Int.* doi:10.1093/gji/ggab236

Badejo, S. A., Muxworthy, A. R., Fraser, A., Stevenson, G. R., Zhao, X., and Jackson, M. (2021b). Identification of magnetic enhancement at hydrocarbon-fluid contacts. *AAPG Bull.* 105, 1973–1991. doi:10.1306/07062019207

Berndt, T., and Muxworthy, A. R. (2017). Dating Icelandic glacial floods using a new viscous remanent magnetization protocol. *Geology* 45, 339–342. doi:10.1130/G38600.1

Berner, R. A. (1967). Thermodynamic stability of sedimentary iron sulfides. *Am. J. Sci.* 265, 773–785. doi:10.2475/ajs.265.9.773

Bilardello, D., Banerjee, S. K., Volk, M. W. R., Soltis, J. A., and Penn, R. L. (2020). Simulation of natural iron oxide alteration in soil: Conversion of synthetic ferrihydrite to hematite without artificial dopants, observed with magnetic methods. *Geochem. Geophys. Geosystems* 21, e2020GC009037. doi:10.1029/2020GC009037

Bleil, U., and Petersen, N. (1982). *Magnetic properties of natural minerals*. Heidelberg, New York: Springer-Verlag, 308–365.

Bleil, U., and Petersen, N. (1983). Variations in magnetization intensity and low-temperature titanomagnetite oxidation of ocean floor basalts. *Nature* 301, 384–388. doi:10.1038/301384a0

Chen, Y., Zhang, W., Nian, X., Sun, Q., Ge, C., Hutchinson, S. M., et al. (2021). Greigite as an indicator for salinity and sedimentation rate change: Evidence from the yangtze river delta, China. *J. Geophys. Res. Solid Earth* 126, 1–16. doi:10.1029/2020JB021085

Collinson, D. W. (1983). *Methods in rock magnetism and palaeomagnetism: Techniques and instrumentation*, 11. New York: Chapman & Hall.

Cunha, A. A., Silva, F. L. d., Silva, B. M. C., Mendes, J. J., Solé, R. A. L., and Araújo, F. G. d. S. (2017). Thermomagnetic study for identification of mineral phases. *Mater. Res.* 20, 125–129. doi:10.1590/1980-5373-MR-2017-0044

Doctor, R., and Feinberg, J. M. (2022). Differential thermal analysis using high temperature susceptibility instruments. *J. Geophys. Res. Solid Earth* 127. doi:10.1029/2021JB023789

Dormann, J.-L., Gasperin, M., and Poullen, J.-F. (1982). Étude structurale de la séquence d'oxydation de la vivianite Fe3(PO4)2.8 H2O. *Bull. Minéralogie* 105, 147–160. doi:10.3406/bulmi.1982.7597

Dunlop, D. J., and Özdemir, Ö. (1997). *Rock magnetism: Fundamentals and Frontiers*. Cambridge University Press.

Emmerton, S. A. (2013). *Investigating the relationship between magnetisation and oil geochemistry*. Ph.D. thesis, Imperial College London

Emmerton, S., Muxworthy, A. R., Sephton, M. A., Aldana, M., Costanzo-Alvarez, V., Bayona, G., et al. (2013). Correlating biodegradation to magnetization in oil bearing sedimentary rocks. *Geochimica Cosmochimica Acta* 112, 146–165. doi:10.1016/j.gca.2013.03.008

Evans, M. E., and Heller, F. (2003). *Environmental magnetism: Principles and applications of enviromagnetics*, 86. San Diego: Academic Press. doi:10.1016/S0074-6142(03)80320-0

Fabian, K., Shcherbakov, V. P., and McEnroe, S. A. (2013). Measuring the Curie temperature. *Geochem. Geophys. Geosystems* 14, 947–961. doi:10.1029/2012gc004440

Frederichs, T., von Dobeneck, T., Bleil, U., and Dekkers, M. (2003). Towards the identification of siderite, rhodochrosite, and vivianite in sediments by their low-temperature magnetic properties. *Phys. Chem. Earth, Parts A/B/C* 28, 669–679. doi:10.1016/S1474-7065(03)00121-9

Frost, R. L., Weier, M. L., Martens, W., Kloprogge, J., and Ding, Z. (2003). Dehydration of synthetic and natural vivianite. *Thermochim. Acta* 401, 121–130. doi:10.1016/S0040-6031(02)00505-1

Gao, X., Hao, Q., Oldfield, F., Bloemendal, J., Deng, C., Wang, L., et al. (2019). New high-temperature dependence of magnetic susceptibility-based climofunction for quantifying paleoprecipitation from Chinese loess. *Geochem. Geophys. Geosystems* 20, 4273–4291. doi:10.1029/2019GC008401

Gehring, A. U., Fischer, H., Louvel, M., Kunze, K., and Weidler, P. G. (2009). High temperature stability of natural maghemite: A magnetic and spectroscopic study. *Geophys. J. Int.* 179, 1361–1371. doi:10.1111/j.1365-246X.2009.04348.x

Gendler, T. S., Shcherbakov, V. P., Dekkers, M. J., Gapeev, A. K., Gribov, S. K., and McClelland, E. (2005). The lepidocrocite-maghemite-haematite reaction chain-i. acquisition of chemical remanent magnetization by maghemite, its magnetic properties and thermal stability. *Geophys. J. Int.* 160, 815–832. doi:10.1111/j.1365-246X.2005.02550.x

Haggerty, S. E. (1991). "Oxide textures - a mini-altas," in *Reviews in mineralogy volume 25 - oxide minerals: Petrologic and magnetic significance*. Editor D. H. Lindsley (Washington D. C.: Mineralogical Society of America).

Heller, F. (1980). Self-reversal of natural remanent magnetisation in the Olby-Laschamp lavas. *Nature* 284, 334–335. doi:10.1038/284334a0

Hodel, F., Macouin, M., Trindade, R. I. F., Araujo, J. F. D. F., Respaud, M., Meunier, J. F., et al. (2020). Magnetic properties of ferritchromite and Cr-magnetite and monitoring of Cr-spinels alteration in ultramafic and mafic rocks. *Geochem. Geophys. Geosystems* 21, e2020GC009227. doi:10.1029/2020GC009227

Hopkinson, J. (1889). XIV. magnetic and other physical properties of iron at a high temperature. *Philosophical Trans. R. Soc. Lond. (A.)* 180, 443–465. doi:10.1098/rsta.1889.0014

Horng, C. S., Chen, J. C., and Lee, T. Q. (1992a). Variations in magnetic minerals from two Plio-Pleistocene marine-deposited sections, Southwestern Taiwan. *J. Geol. Soc. China* 35, 323–335.

Horng, C. S., Laj, C., Lee, T. Q., and Chen, J. C. (1992b). Magnetic characteristics of sedimentary rocks from the tsengwen-chi and erhjen-chi sections in southwestern taiwan. *Terr. Atmos. Ocean. Sci.* 3, 519–532. doi:10.3319/tao.1992.3.4.519(t)

Housen, B. A., Banerjee, S. K., and Moskowitz, B. M. (1996). Low-temperature magnetic properties of siderite and magnetite in marine sediments. *Geophys. Res. Lett.* 23, 2843–2846. doi:10.1029/96GL01197

Hunger, S., and Benning, L. (2007). Greigite: A true intermediate on the polysulfide pathway to pyrite. *Geochem. Trans.* 8, 1–20. doi:10.1186/1467-4866-8-1

Hunt, C. P., Singer, M. J., Kletetshka, G., Tenpas, J., and Verosub, K. L. (1995). Effect of citrate-bicarbonate-dithionite treatment on fine-grained magnetite and maghemite. *Earth Planet. Sci. Lett.* 130, 87–94. doi:10.1016/0012-821X(94)00256-X

Jackson, M., and Bowles, J. (2018). Malleable Curie temperatures of natural titanomagnetites: Occurrences, modes, and mechanisms. *J. Geophys. Res. Solid Earth* 123, 921–940. doi:10.1002/2017JB015193

Jordanova, D., and Jordanova, N. (2016). Thermomagnetic behavior of magnetic susceptibility—Heating rate and sample size effects. *Front. Earth Sci.* 3. doi:10.3389/feart.2015.00090

Kądziałko-Hofmokl, M., Delura, K., Bylina, P., Jeleńska, M., and Kruczyk, J. (2008). Mineralogy and magnetism of Fe–Cr spinel series minerals from podiform chromitites and dunites from Tąpadła (Sudetic ophiolite, SW Poland) and their relationship to palaeomagnetic results of the dunites. *Geophys. J. Int.* 175, 885–900. doi:10.1111/j.1365-246X.2008.03933.x

Kontny, A., de Wall, H., Sharp, T. G., and Pósfai, M. (2000). Mineralogy and magnetic behavior of pyrrhotite from a 260 °C section at the KTB drilling site, Germany. *Am. Mineralogist* 85, 1416–1427. doi:10.2138/am-2000-1010

Krása, D., and Matzka, J. (2007). Inversion of titanomaghemite in oceanic basalt during heating. *Phys. Earth Planet. Interiors* 160, 169–179. doi:10.1016/j.pepi.2006.11.004

Li, H.-Y., and Zhang, S.-H. (2005). Detection of mineralogical changes in pyrite using measurements of temperature-dependence susceptibilities. *Chin. J. Geophys.* 48, 1454–1461. doi:10.1002/cjg2.794

Lin, C. Y., Turchyn, A. V., Krylov, A., and Antler, G. (2019). The microbially driven formation of siderite in salt marsh sediments. *Geobiology* 18, 207–224. doi:10.1111/gbi.12371

Minyuk, P. S., Subbotnikova, T. V., Brown, L. L., and Murdock, K. J. (2013b). High-temperature thermomagnetic properties of vivianite nodules, Lake El'gygytgyn, Northeast Russia. *Clim. Past* 9, 433–446. doi:10.5194/cp-9-433-2013

Minyuk, P. S., Subbotnikova, T. V., and Plyashkevich, A. A. (2011). Measurements of thermal magnetic susceptibility of hematite and goethite. *Izvestiya, Phys. Solid Earth* 47, 762–774. doi:10.1134/S1069351311080052

Minyuk, P., Tyukova, E., Subbotnikova, T., Kazansky, A., and Fedotov, A. (2013a). Thermal magnetic susceptibility data on natural iron sulfides of northeastern Russia. *Russ. Geol. Geophys.* 54, 464–474. doi:10.1016/j.rgg.2013.03.008

Muxworthy, A., and McClelland, E. (2000). The causes of low-temperature demagnetization of remanence in multidomain magnetite. *Geophys. J. Int.* 140, 115–131. doi:10.1046/j.1365-246x.2000.00000.x

Muxworthy, A. R., Heslop, D., Paterson, G. A., and Michalk, D. (2011). A preisach method for estimating absolute paleofield intensity under the constraint of using only isothermal measurements: 2. Experimental testing. *J. Geophys. Res. Solid Earth* 116, B04103. doi:10.1029/2010JB007844

Muxworthy, A. R. (2010). Revisiting a domain-state independent method of palaeointensity determination. *Phys. Earth Planet. Interiors* 179, 21–31. doi:10.1016/j.pepi.2010.01.003

Muxworthy, A. R. (1998). *Stability of magnetic remanence in multidomain magnetite*. Ph.D. thesis, University of Oxford, Oxford.

Nagata, T. (1952). Reverse thermo-remanent magnetism. *Nature* 169, 704–705. doi:10.1038/169704a0

Oches, E. A., and Banerjee, S. K. (1996). Rock-magnetic proxies of climate change from loess-paleosol sediments of the Czech Republic. *Studia Geophys. Geod.* 40, 287–300. doi:10.1007/BF02300744

Ogorodova, L., Vigasina, M., Mel'chakova, L., Rusakov, V., Kosova, D., Ksenofontov, D., et al. (2017). Enthalpy of formation of natural hydrous iron phosphate: Vivianite. *J. Chem. Thermodyn.* 110, 193–200. doi:10.1016/j.jct.2017.02.020

O'Reilly, W. (1976). Magnetic minerals in the crust of the Earth. *Rep. Prog. Phys.* 31, 857–908. doi:10.1088/0034-4885/39/9/002

Özdemir, Ö., and Dunlop, D. J. (2000). Intermediate magnetite formation during dehydration of goethite. *Earth Planet. Sci. Lett.* 177, 59–67. doi:10.1016/S0012-821X(00)00032-7

Özdemir, Ö., and Dunlop, D. J. (2005). Thermoremanent magnetization of multidomain hematite. *J. Geophys. Research-Solid Earth* 110. doi:10.1029/2005JB003820

Özdemir, Ö. (1990). High-temperature hysteresis and thermoremanence of single-domain maghemite. *Phys. Earth Planet. Inter.* 65, 125–136. doi:10.1016/0031-9201(90)90081-8

Özdemir, Ö. (1987). Inversion of titanomaghemites. *Phys. Earth Planet. Interiors* 46, 184–196. doi:10.1016/0031-9201(87)90181-6

Perkins, J. R. (2022). "Hydrocarbon source and migration pathway identification through basin and petroleum systems modelling and mineral magnetism: A case study on the beatrice field," in *Inner Moray Firth* (UK North Sea: Ph.D. thesis, Imperial College London).

Perkins, J. R., Muxworthy, A. R., Fraser, A., and Hu, P. (2023). UK North Sea. submitted.Quantifying the mineral magnetic signature of petroleum systems and their source rocks: A study on the inner Moray Firth. *Geophys. J. Int.*

Petersen, N. (1984). *Ore mineralogy of south atlantic basalts (Deep Sea Drilling Project Leg 73)*, 73. Washington, D.C.: U.S. Government Printing Office. doi:10.2973/dsdp.proc.73.122.1984

Petrovský, E., and Kapička, A. (2006). On determination of the Curie point from thermomagnetic curves. *J. Geophys. Res. Solid Earth* 111. doi:10.1029/2006JB004507

Pye, K. (1981). Marshrock formed by iron sulphide and siderite cementation in saltmarsh sediments. *Nature* 294, 650–652. doi:10.1038/294650a0

Roberts, A. P., Chang, L., Rowan, C., Horng, C.-S., and Fabio, F. (2011). Magnetic properties of sedimentary greigite (Fe_3S_4): An update. *Rev. Geophys.* 49, RG1002–46. doi:10.1029/2010RG000336

Roberts, A. P. (2015). Magnetic mineral diagenesis. *Earth Sci. Rev.* 151, 1–47. doi:10.1016/j.earscirev.2015.09.010

Roberts, A. P., and Weaver, R. (2005). Multiple mechanisms of remagnetization involving sedimentary greigite (Fe_3S_4). *Earth Planet. Sci. Lett.* 231, 263–277. doi:10.1016/j.epsl.2004.11.024

Rochette, P., Fillion, G., Mattéi, J.-L., and Dekkers, M. J. (1990). Magnetic transition at 30–34 kelvin in pyrrhotite: Insight into a widespread occurrence of this mineral in rocks. *Earth Planet. Sci. Lett.* 98, 319–328. doi:10.1016/0012-821X(90)90034-U

Rodgers, K. A., and Henderson, G. S. (1986). The thermochemistry of some iron phosphate minerals: Vivianite, metavivianite, baraćite, ludlamite and vivianite/metavivianite admixtures. *Thermochim. Acta* 104, 1–12. doi:10.1016/0040-6031(86)85179-6

Rothe, M., Kleeberg, A., Grüneberg, B., Friese, K., Pérez-Mayo, M., and Hupfer, M. (2015). Sedimentary sulphur:iron ratio indicates vivianite occurrence: A study from two contrasting freshwater systems. *PLoS One* 10, e0143737. doi:10.1371/journal.pone.0143737

Schwarz, E. J., and Vaughan, D. J. (1972). Magnetic phase relations of pyrrhotite. *J. geomagnetism Geoelectr.* 24, 441–458. doi:10.5636/jgg.24.441

Snowball, I., and Thompson, R. (1988). The occurrence of greigite in sediments from loch lomond. *J. Quat. Sci.* 3, 121–125. doi:10.1002/jqs.3390030203

Sprain, C. J., Feinberg, J. M., Renne, P. R., and Jackson, M. (2016). Importance of titanohematite in detrital remanent magnetizations of strata spanning the Cretaceous-Paleogene boundary, Hell Creek region, Montana. *Geochem. Geophys. Geosystems* 17, 660–678. doi:10.1002/2015gc006191

Till, J. L., and Nowaczyk, N. (2018). Authigenic magnetite formation from goethite and hematite and chemical remanent magnetization acquisition. *Geophys. J. Int.* 213, 1818–1831. doi:10.1093/gji/ggy083

Turney, J. N., Weiss, D., Muxworthy, A. R., and Fraser, A. (2023). Greigite formation in aqueous solutions: Critical constraints into the role of iron and sulphur ratios, pH and eh, and temperature using thermodynamic reaction process modelling. *Chem. Geol.* in press.

Wang, L., Pan, Y., Li, J., and Qin, H. (2008). Magnetic properties related to thermal treatment of pyrite. *Sci. China Ser. D Earth Sci.* 51, 1144–1153. doi:10.1007/s11430-008-0083-7